Thermally induced dephasing in periodically poled KTP frequency-doubling crystals

Zhi M. Liao, Stephen A. Payne, Jay Dawson, Alex Drobshoff, Chris Ebbers, and Dee Pennington

Lawrence Livermore National Laboratory, 7000 East Avenue, L-482, Livermore, California 94550

Luke Taylor

European Southern Observatory, Karl-Schwarzschild-Strasse 2, Garching D85748, Germany

Received December 8, 2003; revised manuscript received June 9, 2004; accepted July 13, 2004

A thermally induced spatial and temporal dephasing model of second-harmonic generation has been developed to describe the conversion efficiency and its degradation of periodically poled potassium titanium phosphate (PPKTP) in a cw, single-pass frequency conversion system. The model confirms the experimental data that show that second-harmonic power greater than 800 mW (15 kW/cm^2) causes two-photon nonlinear absorption, leading to time-dependent photochromic damage in PPKTP. This added absorption degrades the conversion efficiency from an initial value of 19% to an unrecoverable asymptotic value of ~8% in 2 h at 145 kW/cm^2 of pump intensity through thermal detuning phase mismatch. © 2004 Optical Society of America

OCIS codes: 190.0190, 190.2620, 190.4360, 190.4400.

1. INTRODUCTION

Periodically poled nonlinear materials have the potential to serve as versatile devices for laser developers because of their ability to quasi-phase match (QPM) over long lengths of crystal and allow noncritical phase matching for tight focusing geometries, thereby enabling efficient frequency conversion of cw lasers. A number of crystals have been successfully poled for frequency conversion,[1–5] of which periodically poled $LiNbO_3$ and periodically poled potassium titanium phosphate (PPKTP) have produced the most success. Periodically poled $LiNbO_3$ has demonstrated high conversion efficiency (2.7 W out of 6.5 W) in cw single-pass operation before exhibiting photorefractive damage.[6] Recently, periodically poled stoichiometric $LiTaO_3$ has successfully demonstrated 300 min of cw single-pass second-harmonic generation (SHG) at 1064 nm (1.6 W out of 18 W) without observable damage.[7] Unfortunately, there have been no reported cw high-power studies by use of PPKTP, although no damage was observed in the low-power regime (approximately milliwatts).[8] In pulsed systems, however, PPKTP has been shown to be capable of generating large amounts of 532-nm light (up to 6 W averaged power)[9] as well as to obtain high efficiency (>65% peak conversion) without observing degradation.[10]

In bulk KTP crystals, laser intensity-induced damage (gray tracking) is well documented.[11–15] The transmission degradation of the crystal across visible wavelengths generally contributes to the creation of color centers through two-photon absorption. We describe our assessment of time-dependent conversion efficiency degradation in PPKTP in a cw single-pass configuration. In addition, we propose a model based on photochromic damage that is due to the creation of color centers by means of two-photon absorption. We found that the temperature rise in the focal region (from induced absorption) rather than direct absorption loss is the cause of the degradation.

2. THEORY

The exact treatment of SHG consisted of solving the coupled-wave equation of the pump and the signal fields as it propagates through the crystal.[16,17] There have been several papers that reported on the reduction of a coupled-wave equation to a closed-form analytical solution. Most notably Armstrong *et al.*[18] solved the coupled-wave equation analytically by transforming it into the form of elliptical integrals. Their analysis is valid only in the weak or confocal focusing limit, i.e., $L < b$, where L is the crystal length and $b = kw_0^2$ (k is the wave number and w_0 is the beam waist of a Gaussian beam) is the confocal parameter of the beam. The beam is assumed to have the same waist and therefore the same power intensity throughout the crystal. Boyd and Kleinman[19] expanded beyond the confocal regime by explicitly taking into account the propagation of the Gaussian beam inside the crystal and numerically calculating the optimal focusing condition under strong focusing. Their analysis for the QPM process resulted in a single maxima for frequency conversion, $L = 2.84b$, which can serve as an upper bound for nonlinear frequency conversion.

The solution of SHG in the Boyd and Kleinman focusing regime is given as

$$P_{2\omega} = fgL\,\eta P_{1\omega}^2, \tag{1}$$

where f is the focusing factor that accounts for nonideal focusing, g is the nonlinear conversion coefficient, η is the thermal dephasing factor averaged over the crystal length, and $P_{1\omega}$ and $P_{2\omega}$ are the fundamental and the

second-harmonic powers, respectively. The nonlinear conversion coefficient is given by

$$g = \frac{2H\omega_1{}^3 d_q{}^2}{\pi\epsilon_0 c^4 n_1 n_2}, \tag{2}$$

where H is the numerically calculated focusing enhancement factor that depends on the ratio b/L,[19] ω_1 is the pump frequency, d_q is the effective QPM nonlinear coefficient, ϵ_0 is the permittivity of free space, c is the speed of light, and n_1 and n_2 are the indices of the crystal at the fundamental and second-harmonic frequencies, respectively.

Thermal dephasing factor η is a function of temperature detuning (ΔT) and is given by[17]

$$\eta(\Delta T) = \mathrm{sinc}^2\left(\frac{\beta_T L}{2}\Delta T\right), \tag{3}$$

where β_T is the temperature-dependent phase mismatch. Temperature detuning caused by the local heating of an intensely focused beam that is cooled on the side can be taken into account by solving Poisson's equation.[20] The temperature difference between the center and the edge of the crystal aperture that is due to absorption of the optical intensity to first order (assuming circular symmetric) is

$$\Delta T = \frac{\alpha P}{4\pi K}\left[1 + 2\ln\left(\frac{a}{w_0}\right)\right], \tag{4}$$

where a is the width of the crystal, α is the absorption coefficient, P is the optical power, and K is the thermal conductivity. The value of absorption is a time-dependent quantity that is due to the defect absorption induced by the second-harmonic beam.

The process of defect creation and bleaching is a well-documented effect in many crystals,[21,22] and the canonical form that describes this process can be written as

$$\frac{\mathrm{d}N}{\mathrm{d}t} = \beta I^2 (N_s - N), \tag{5}$$

where the defect density is N, β is the defect-creation coefficient, N_s is the steady-state defect density, and I is the intensity of the defect-generation beam. Here we assume that the defects are formed by activating precursors present in the crystal. Defect generation is a function of I^2 because the process is a two-photon absorption interaction.[15] We can relate the nonlinear two-photon absorption to the defect (or color center) density by $\alpha_N = \sigma N$, where σ is the cross section of the defects. The expression for nonlinear absorption as a function of time then becomes

$$\alpha_N(t) = \alpha_s[1 - \exp(-\beta I^2 t)], \tag{6}$$

where α_s becomes the steady-state or saturated nonlinear absorption.

The total absorption of the crystal is then the sum of the linear absorption (α_L) that is due to impurities and the time-dependent nonlinear absorption (α_N) that is due to precursor defects $\alpha = \alpha_L + \alpha_N(t)$. Furthermore, studies of the wavelength dependence of nonlinear absorption in KTP have indicated that the nonlinear absorption coefficient is stronger at shorter wavelengths and decreases monotonically as the wavelength increases.[11,14] The relative measurement of nonlinear absorption at the absorption peak of 400 nm is almost a factor of 10 stronger than the longest wavelength study at 800 nm.[14] As a result, the dominating radiation responsible for nonlinear absorption is the second-harmonic light. Combining Eqs. (1)–(5) yields a time-dependent transcendental equation that takes into account thermally induced dephasing from the temperature rise that is due to nonlinear absorption. Finally, an alignment factor (δT) that accounts for the initial nonoptimal QPM temperature setting is added to the full model as follows:

$$P_{2\omega} = fgP_{1\omega}{}^2 \mathrm{sinc}^2\left[\frac{\beta_T L}{2}\left(\frac{1 + 2\ln(a/w_0)}{4\pi K} \times \{\alpha_L + \alpha_s[1 - \exp(-\beta I_{2\omega}{}^2 t)]\}P_{2\omega} + \delta T\right)\right] \times \left[\frac{1 - \exp(-\{\alpha_L + \alpha_s[1 - \exp(-\beta I_{2\omega}{}^2 t)]\}L)}{\alpha_L + \alpha_s[1 - \exp(-\beta I_{2\omega}{}^2 t)]}\right]. \tag{7}$$

The first factor accounts for nonlinear conversion, the second factor accounts for reduction of second-harmonic light that is due to dephasing, and the last factor is the effective crystal length that adjusts to the loss of second-harmonic light that is due to absorption. Heating is actually a function of varying beam waist, which here we treat as a lumped parameter. This averaged dephasing model is therefore valid only when the dephasing is small enough throughout the crystal length to create only a perturbative dephasing. A large local dephasing can effectively chirp the grating, in which case, a full coupled-wave equation treatment would be required to model the system response accurately.

3. EXPERIMENT

The experimental setup for SHG testing is shown in Fig. 1. A 1064-nm Cutting Edge Optronics pump module is used as the pump source along with an intercavity aperture to obtain a near single transverse mode ($M^2 = 1.1$ as measured with a Coherent mode master). A polarizer is placed immediately outside the cavity to obtain the correct polarization state. Since the cavity is extremely sensitive to the drive current because of thermal lensing of the pump module, a polarizer and a half-wave plate were used to vary the incident power on the crystal. The Raicol Crystals (Israel) flux-grown PPKTP has a dimension of 1 mm × 2 mm × 30 mm and a period of 9.1 μm for a calculated phase-matched temperature of 148 °C for SHG to 532 nm. The crystal is wrapped in thin foil, which is

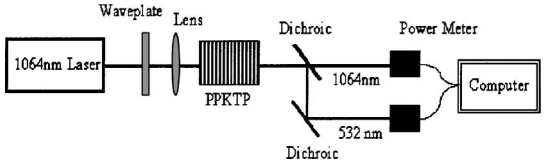

Fig. 1. Experimental setup.

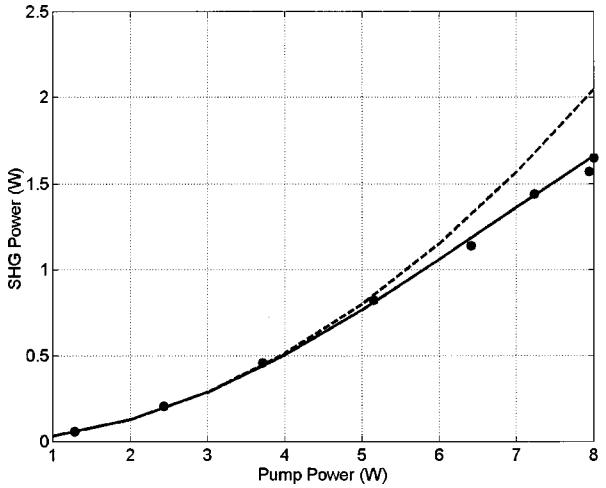

Fig. 2. Experimental (filled circle) and predicted (solid curve) SHG power as a function of pump power. Dashed curve represents the predicted SHG power without dephasing effects ($\alpha_L = 0$).

in contact with the oven. Different lens systems were used to obtain various peak pump intensities to study the effects of confocal and strong focusing. The second-harmonic power was separated from the residual pump power by use of two dichroics that are designed to pass the 1064-nm light and reflect the 532-nm light. Power as a function of time from both wavelengths was monitored with powermeters interfaced to a PC. Optimal adjustment of the crystal position, temperature setting, and the wave plate is performed at the beginning of each measurement for a given pump power.

The first set of data taken (dots) consists of input power versus output SHG power as shown in Fig. 2. The pump beam is carefully realigned to the crystal for each data point; the values were taken within minutes of optimizing the alignment. The theoretical fit (solid curve) is based on our model as described in Eq. (7). The parameter values used for the calculation are given in Table 1 with parameters f and α_L used to account for the focusing factor and the effect of linear absorption, respectively. Theoretical calculations of SHG power without the dephasing effect (dashed curve) clearly shows a pump threshold power of ~5 W in which the dephasing effect starts to become prominent.

Long-term testing of the frequency conversion at high pump ($P_{1\omega} = 6.8$ W) power reveals degradation of the SHG power as a function of time (see Fig. 3). The parameters used to fit the data were nonlinear absorption α_s and defect creation rate β (see Table 1). The power was observed to degrade exponentially to a nonzero, steady-state value. The rate at which the SHG power degrades was observed to increase with an increase in pump power although the steady-state SHG conversion efficiency remains similar. We then carried out a comprehensive series of time-series measurements with various input powers to validate the model (see Fig. 4). For each input power, the alignment procedure was repeated at a different spot in the crystal to ensure that the alignment was started at fresh spots. SHG power and residual pump power were recorded for 25 min. For the theoretical calculations, all the parameters were already set from the previous two data sets (see Figs. 2 and 3) so only the alignment factor δT was adjusted for each data series. The alignment factor depends primarily on improper setting of the optimal temperature for the oven; the values we used ranged from 0 to 0.4 °C. Similar to Fig. 2, a pump threshold of 5 W that translates to a SHG threshold of 800 mW is clearly evident above which degradation of the SHG power starts to take effect.

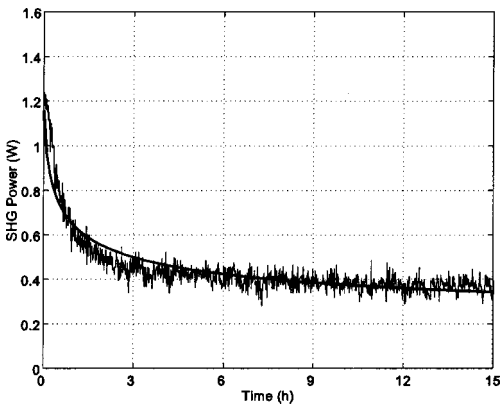

Fig. 3. Experimental (dashed curve) and theoretical (solid curve) SHG power versus time with $P_{1\omega} = 6.8$ W.

Table 1. Parameters Used for the Theoretical Calculations

Parameter Name	Symbol	Value	Reference
Focusing fit	f	0.75	Fit from Fig. 2
Nonlinear coefficient	d_q	9.5 pV/m	Literature report
Index at pump	n_1	1.7381	Sellmeier calculation[23]
Index at signal	n_2	1.7785	Sellmeier calculation[23]
Thermal conductivity	K	3 W/C/m	Literature report[23]
Crystal width	a	1 mm	Laboratory measurement
Focused spot	w_0	42 μm	Laboratory measurement
Crystal length	L	30 mm	Laboratory measurement
Temperature-dependent mismatch	β_T	1.47 rad/°C	Laboratory measurement
Focusing enhancement	H	1	See Ref. 19
Linear absorption	α_L	1%/cm	Fit from Fig. 2
Saturated absorption	α_s	14%/cm	Fit from Fig. 3
Defect creation	β	3.75×10^3 μm^4/W^2/s	Fit from Fig. 3

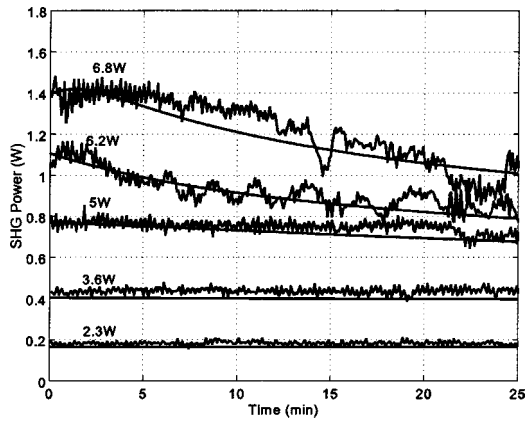

Fig. 4. Experimental (dotted curve) and theoretical (solid curve) SHG power versus time for various input powers. Alignment factors δT were 0, −0.1, −0.1, 0, −0.4 °C from low to high powers.

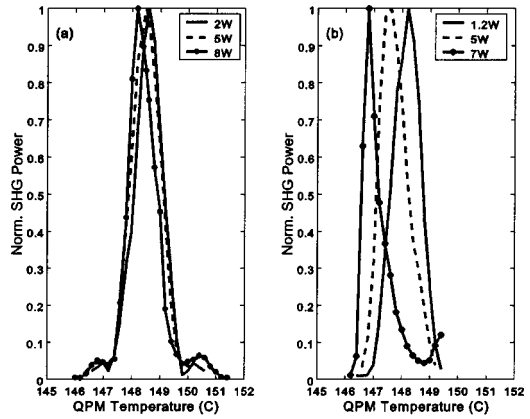

Fig. 5. Temperature tuning curve for different input powers for (a) undamaged and (b) damaged spots.

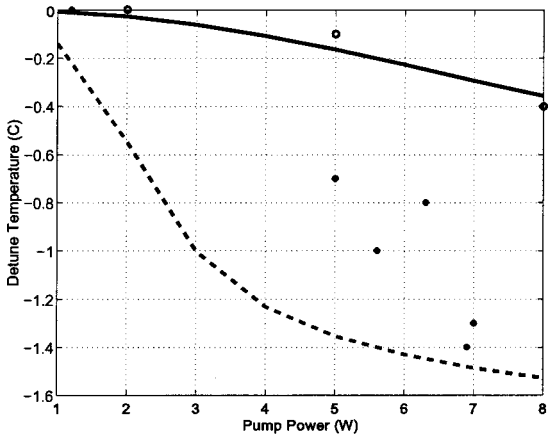

Fig. 6. Measured (symbols) and calculated (curves) QPM temperature detuning as a function of pump power before damage (open circles, solid curve) and after damage (filled circles, dashed curve).

Although pump–probe absorption measurements can directly validate the absorption,[24] an indirect confirmation of the thermally induced dephasing mechanism can be obtained by measurement of the phase-matching temperature for various input power levels before and after steady-state damage occurs since the absorption can be linked to the temperature rise directly through Eq. (4). This can be accomplished by taking the temperature versus the SHG power curve before and after damage at different input powers (see Fig. 5). The optimal phase-matching temperature can then be plotted along with the calculated temperature rise that is strictly due to linear absorption [undamaged spot, Fig. 5(a)] and total absorption, which includes saturated nonlinear absorption [damaged spot, Fig. 5(b)] by use of Eq. (4). No additional parameters were adjusted to obtain the fits in Fig. 6.

4. DISCUSSION

Even when the power was measured instantaneously as in Fig. 2, it is evident that there is a threshold pump power above which degradation starts to occur. This pump power corresponds to an intensity of 90 kW/cm^2 from 5 W with $w_0 \sim 42\,\mu$m. When the beam was focused loosely corresponding to the confocal regime ($w_0 \sim 57\,\mu$m), no degradation was observed even at 8 W of pump power (78 kW/cm^2). This is clearly displayed in Fig. 7, where the SHG intensity is plotted versus pump intensity for confocal focusing ($w_0 \sim 57\,\mu$m) and strong focusing ($w_0 \sim 42\,\mu$m). Figure 7 shows that even at the highest available pump power, the SHG power density is still below the damage threshold for loose or confocal focusing, therefore conversion roll-off was not observed, confirming that the effect is due to intensity not power. This agrees with our model since we assume that it is the absorption of SHG light that causes the roll-off and the amount of SHG generated is related to the intensity of the pump. In addition, the conversion degradation was not observed when the pump was not in the correct polarization. Furthermore, linear absorption measured at 532 nm (1%/cm) is 100 times greater than that at 1064 nm (0.01%/cm),[25] so even at 20% conversion, absorption at 532-nm light is still the dominating contributor.

The fact that a similar threshold existed when the time-dependent measurements were taken (see Fig. 4) is a strong indication that a similar mechanism is at work—degradation that is due to dephasing through linear and nonlinear absorption. The conversion efficiency decays

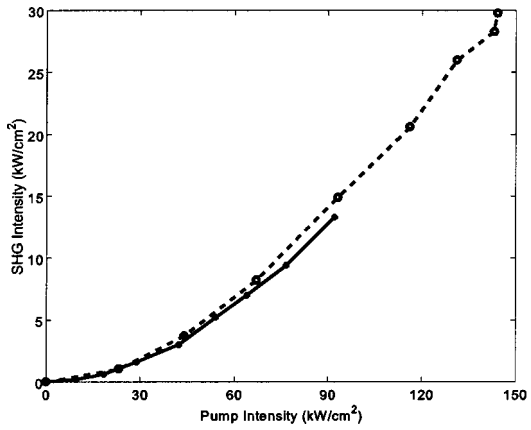

Fig. 7. SHG intensity versus pump intensity for confocal focusing (solid curve, $w_0 = 57\,\mu$m) and strong focusing (dashed curve, $w_0 = 42\,\mu$m).

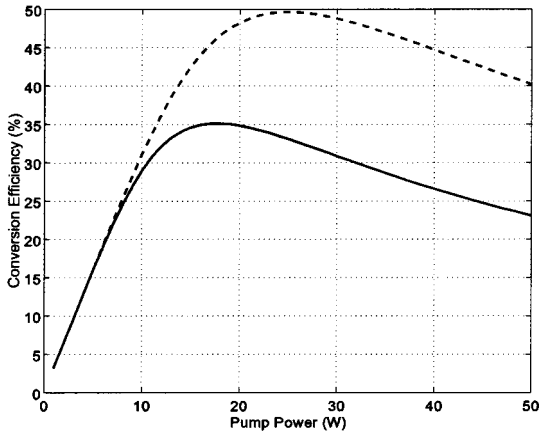

Fig. 8. Theoretical calculated conversion efficiency versus pump power at $t = 0$ (dashed curve) and $t = 1000$ h (solid curve) for hydrothermal PPKTP with $\alpha_L = \alpha_s = 0.22\%/\text{cm}$.

to an asymptotic value that translates to a maximum precursor site concentration. The time characteristics of defect or color-center creation match well with gray tracking of bulk KTP that has undergone damage-protective treatment by Murk *et al.*[12] The saturation time is of the order of 2 h but, unlike for the bulk KTP results,[12,14] we were unable to produce any defect decay after 2–3 days even after the crystal was annealed at $T \sim 500$ K. It is unclear from the data whether the observed difference is attributed to the cw operation and/or the periodic poling of the material itself. No significant changes in the pump or the SHG beam profiles were observed in the damaged versus undamaged regime. Furthermore, once the damage was initiated, there was no degradation in the conversion efficiency when running below the threshold level. In addition, conversion degradation occurs only above the threshold intensity, strongly indicating that the degradation is due to dephasing as opposed to actual physical damage. The fact that our theoretical calculation predicts the temperature detuning quantitatively (see Fig. 6) further reinforces the accuracy of the model. It is evident from Fig. 5(b) that the temperature-tuning curve of the damaged spot at high power (7 W) is highly asymmetric and began to deviate strongly from the sinc-squared characteristics. This indicates that the absorption-induced dephasing might have started to chirp the grating structure, which exceeds the validity of the current lumped dephasing model.

It is worthwhile to note that there is no easy way to overcome this deficiency. Since the contributing factor is the second-harmonic intensity, this essentially limits how much second-harmonic light can be stably produced. Reformatting the beam to large spot sizes would hamper the overall conversion efficiency unless longer crystals can be obtained; even then, this would only prolong the decay rate. It would take longer to get to the saturation point, but the saturation point would be the same unless a higher quality crystal could be obtained. As a result, only by producing a purer quality crystal with reduced precursor density can this be overcome. Given a hydrothermally grown (or gray track resistant) KTP, with linear absorption reduced from 1%/cm to 0.22%/cm,[25] our model predicts that, with similar focusing geometry, upward of 35% conversion efficiency could be obtained stably if the saturated nonlinear absorption were also reduced to that of 0.22%/cm (see Fig. 8).

5. CONCLUSION

We have presented experimental data on conversion efficiency degradation in a single-pass, cw SHG system by using PPKTP. We have also presented in detail a successful model based on spatial–temporal thermally induced dephasing through local heating. The generation of defect sites leads to nonlinear absorption that is found to be unrecoverable and is activated by a two-photon absorption of the 532-nm light at a threshold power of 800 mW (15 kW/cm^2).

ACKNOWLEDGMENT

The authors thank D. Bonaccini and W. Hackenberg of the European Southern Observatory for helpful discussions and valuable equipment; Ray Beach, Keith Kanz, and Randy Bonner for help with the laser. This research was done under the auspices of the U.S. Department of Energy by the University of California Lawrence Livermore National Laboratory (LLNL) under contract W-7405-ENG-48 and funded through the LLNL office of Laboratory Directed Research and Development (01-ERD-83) and the National Science Foundation Center for Adaptive Optics.

Z. M. Liao's e-mail address is liao2@llnl.gov.

REFERENCES

1. Y. Xue, N. Ming, J. Zhu, and D. Feng, "The second harmonic generation in $LiNbO_3$ crystals with period laminar ferroelectric domains," Chin. Phys. **4**, 554–564 (1984).
2. W. Wang, Q. Zhou, Z. Geng, and D. Feng, "Study of $LiTaO_3$ crystals grown with a modulated structure. I. Second harmonic generation in $LiTaO_3$ crystals with periodic laminar ferroelectric domains," J. Cryst. Growth **79**, 706–709 (1986).
3. Q. Chen and W. P. Risk, "Periodic poling of $KTiOPO_4$ using an applied electric field," Electron. Lett. **30**, 1516–1517 (1994).
4. H. Karlsson, F. Laurell, P. Henriksson, and G. Arvidsson, "Frequency doubling in periodically poled $RbTiOAsO_4$," Electron. Lett. **32**, 556–557 (1996).
5. A. Chowdhury, H. M. Ng, M. Bhardwaj, and N. G. Weimann, "Second-harmonic generation in periodically poled GaN," Appl. Phys. Lett. **83**, 1077–1079 (2003).
6. G. D. Miller, R. G. Batchko, W. M. Tulloch, D. R. Weise, M. M. Fejer, and R. L. Byer, "42%-Efficient single-pass cw second-harmonic generation in periodically poled lithium niobate," Opt. Lett. **22**, 1834–1836 (1997).
7. M. Katz, R. Route, D. Hum, R. Roussev, K. Parameswaran, V. Kondilenko, G. Miller, and M. Fejer, "Near-stoichiometric 1% Mg-doped $LiNbO_3$ and stoichiometric $LiTaO_3$ fabricated by vapor transport equilibration for frequency conversion," in *Stanford Photonics Research Center Annual Report* (Stanford Photonics Research Center, Stanford, Calif., 2003).
8. A. Arie, G. Rosenman, V. Mahal, A. Skliar, M. Oron, M. Katz, and D. Eger, "Green and ultraviolet quasi-phase-matched second harmonic generation in bulk periodically-poled $KTiOPO_4$," Opt. Commun. **142**, 265–268 (1997).
9. S. V. Popov, S. V. Chernikov, and J. R. Taylor, "6-W Average power green light generation using seeded high power yt-

terbium fibre amplifier and periodically poled KTP," Opt. Commun. **174**, 231–234 (2000).
10. V. Pasiskevicius, S. Wang, J. A. Tellefsen, F. Laurell, and H. Karlsson, "Efficient Nd:YAG laser frequency doubling with periodically poled KTP," Appl. Opt. **37**, 7116–7119 (1998).
11. V. A. Maslov, V. A. Mikhailov, O. P. Shaunin, and I. A. Shcherbakov, "Nonlinear absorption in KTP crystals," Quantum Electron. **27**, 356–359 (1997).
12. V. Mürk, V. Denks, A. Dudelzak, P. Proulx, and V. Vassiltsenko, "Gray tracks in $KTiOPO_4$: mechanism of creation and bleaching," Nucl. Instrum. Methods Phys. Res. B **141**, 472–476 (1998).
13. X. Mu, Y. J. Ding, J. Wang, Y. Liu, J. Wei, and J. B. Khurgin, "Damage mechanisms for $KTiOPO_4$ crystals under irradiation of a cw argon laser," in *Laser Material Crystal Growth and Nonlinear Materials and Devices*, K. I. Schaffers and L. E. Myers, eds., Proc. SPIE **3610**, 9–14 (1999).
14. B. Boulanger, I. Rousseau, J. P. Feve, M. Maglione, B. Menaert, and G. Marnier, "Optical studies of laser-induced gray-tracking in KTP," IEEE J. Quantum Electron. **35**, 281–286 (1999).
15. B. Boulanger, J.-P. Fève, and Y. Guillien, "Thermo-optical effect and saturation of nonlinear absorption induced by gray tracking in a 532-nm-pumped KTP optical parametric oscillator," Opt. Lett. **25**, 484–486 (2000).
16. R. Boyd, *Nonlinear Optics* (Academic, San Diego, Calif., 1992).
17. M. M. Fejer, G. A. Magel, D. H. Jundt, and R. L. Byer, "Quasi-phase-matched second harmonic generation: tuning and tolerances," IEEE J. Quantum Electron. **28**, 2631–2654 (1992).
18. J. A. Armstrong, N. Bloembergen, J. Ducuing, and P. S. Pershan, "Interactions between light waves in a nonlinear dielectric," Phys. Rev. **127**, 1918–1939 (1962).
19. G. D. Boyd and D. A. Kleinman, "Parametic interaction of focused Gaussian light beams," J. Appl. Phys. **39**, 3597–3639 (1968).
20. D. Eimerl, "Thermal aspects of high-average-power electrooptic switches," IEEE J. Quantum Electron. **23**, 2238–2251 (1987).
21. A. J. Bayramian, C. D. Marshall, J. H. Wu, J. A. Speth, S. A. Payne, G. J. Quarles, and V. K. Castillo, "Ce:$LiSrAlF_6$ laser performance with antisolarant pump beam," J. Lumin. **69**, 85–94 (1996).
22. C. D. Marshall, S. A. Payne, M. A. Henesian, J. A. Speth, and H. T. Powell, "Ultraviolet-induced transient absorption in potassium dihydrogen phosphate and its influence on frequency conversion," J. Opt. Soc. Am. B **11**, 774–785 (1994).
23. Eksma Co. KTP product specification, www.eksma.lt, Vilnius, Lithuania.
24. A. A. Alexandrovski, G. Foulon, L. E. Myers, R. K. Route, and M. M. Fejer, "UV and visible absorption in $LiTaO_3$," in *Laser Material Crystal Growth and Nonlinear Materials and Devices*, K. I. Schaffers and L. E. Myers, eds., Proc. SPIE **3610**, 44–51 (1999).
25. Cristal Laser KTP product specification, www.cristal-laser-fr, Chaligny, France.